In vitro and *in vivo* growth inhibition and G_1 arrest in human cancer cell lines by diaminophenyladamantane derivatives

Jane-Jen Wang[a], Yu-Chen Chen[b], Chin-Wen Chi[b,c], Kuo-Tong Huang[d] and Yaw-Terng Chern[e]

We describe the discovery of a novel series of anticancer adamantane derivatives which induce G_1 arrest in Colo 205 and HT 29 colon cancer cells. Seven adamantane derivatives were screened for their activity *in vitro* against 60 human cancer cell lines in the National Cancer Institute (NCI)'s Anticancer Drug Screen system. The relationships between structure and *in vitro* anticancer activity are discussed. 1,3-Bis(4-(4-amino-3-hydroxyphenoxy) phenyl)adamantane (1,3-DPA/OH/NH_2) and 2,2-bis (4-(4-amino-3-hydroxyphenoxy)phenyl)adamantane (DPA) exhibited strong growth inhibitory on anticancer activities *in vitro*. The IC_{50}s of 1,3-DPA/OH/NH_2 (NSC-706835) and DPA (NSC-706832) were found to be $<3\,\mu M$ against 45 (85%) and 48 (91%) cell lines, respectively. 2,2-Substituted adamantane derivatives exhibited stronger growth inhibition on anticancer activities *in vitro* than the corresponding 1,3-subsitituted analogs. Very strong growth inhibition of 2,2-bis(4-aminophenyl)adamantane (NSC-711117) was observed against two colon cancer lines (HT-29 and KM-12), one CNS cancer line (SF-295) and one breast cancer line (NCI/ADR-RES) with $IC_{50}<1.0\,\mu M$, i.e. 0.1, 0.01, 0.059 and $0.079\,\mu M$, respectively. In addition, we also examined the *in vitro* and *in vivo* effects of DPA on three human colon cancer cells. DPA-treated Colo 205 and HT-29 cells were arrested at G_0/G_1 as analyzed by flow cytometric analysis. The DPA-induced cell growth inhibition was irreversible after removal of DPA. The *in vivo* effect of tumor growth suppression by DPA was also observed on colon Colo 205 xenografts. No acute toxicity was observed after an i.p. challenge of DPA in ICR nude mice weekly. These results suggest that DPA appears to be a new potentially less toxic modality of cancer therapy. *Anti-Cancer Drugs* 15:697–705 © 2004 Lippincott Williams & Wilkins.

Anti-Cancer Drugs 2004, **15**:697–705

Keywords: adamantane, anticancer activity, G_1 arrest

[a]National Taipei College of Nursing, Taipei, Taiwan, [b]Institute of Pharmacology, School of Medicine, National Yang-Ming University, Taipei, Taiwan, [c]Department of Medical Research and Education, Taipei Veterans General Hospital, Taipei, Taiwan, [d]Department of Internal Medicine, National Taiwan University Hospital, Taipei, Taiwan and [e]Department of Chemical Engineering, National Taiwan University of Science and Technology, Taipei, Taiwan.

Correspondence to Y.-T. Chern, Department of Chemical Engineering, National Taiwan University of Science and Technology, 43, Keelung Road, Section 4, Taipei 106, Taiwan.
Tel: +886-273 76646; fax: +886-273 76644;
e-mail: cyt@ch.ntust.edu.tw

Received 17 January 2004 **Revised form accepted** 16 April 2004

Introduction

Colon cancer is a major cause of mortality in the Western world [1]. Although chemotherapy and radiation therapy have been attempted in either adjuvant or palliative treatments, more effective adjuvant therapy is needed for colon cancer patients. Nearly half of all patients with colon cancer still die of metastatic disease after curative surgery [2]. Thus, developing new therapeutic drugs or techniques for colon cancer is a worthwhile task. Malignant tumor cells are clearly distinguished from normal cells by their chaotic proliferation due to a serious disorder of the cell cycle regulatory machinery. Cell cycle inhibitors or modulators that halt uncontrollable tumor growth are regarded as highly promising new therapeutic agents on human cancers [3]. Recent studies have shown that the G_1 phase of the cell cycle is an important period where various signals interact to determine the proliferation, quiescence, differentiation or apoptosis of cells [4,5]. The use of chemical agents to induce differentiation of tumor cells has received widespread attention as a potentially less toxic cancer therapy.

Adamantane derivatives possess several attractive pharmacological activities such as antibacterial, antifungal, antiviral and anticancer effects [6–8]. Therefore many investigators consider them as highly promising candidates in drug design [9–11]. For example, the aminoadamantane derivatives memantine (1-amino-3,5-dimethyladamantane) and amantadine (1-aminoadamantane) are uncompetitive *N*-methyl-D-aspartate (NMDA) receptor antagonists which have been used clinically in the treatment of dementia and Parkinson's disease for several years without serious side effects [9,10]. Our previous study has found that *N*-1-adamantylmaleimide (AMI) and dimethyladamantylmaleimide (DMAMI) induce apoptosis and inhibit the growth of the human gastric (SC-M1) and colon (Colo 205) cancer in SCID mice, respectively [12,13]. In a recent study we have characterized the anticancer activities of diaminodiamantane derivatives

0959-4973 © 2004 Lippincott Williams & Wilkins DOI: 10.1097/01.cad.0000136881.42423.98

using the 60 human cancer cell lines in the NCI Anticancer Drug Screen and evaluated the structure–activity relationship. 1,6-Bis(4-(4-amino-3-hydroxyphenoxy)phenyl)diamantane (DPD) exhibited marked anticancer activities on the colon cancer cell lines [14]. We have recently demonstrated that administration of DPD induced G_0/G_1 arrest and differentiation in human colon cancer cells [15]. DPD also shows *in vivo* anticancer activity on human colon cancer cells xenografts with no obvious acute toxicity [15]. Adamantane and diamantane are closely analogous polycyclic alkanes with the structure of three and six fused cyclohexane rings, respectively. From these results we hypothesize that DPA shows anticancer effects against human colon cancer cells. To the best of our knowledge, the present study is the first report that refers to the anticancer activities of diaminophenyladamantane derivatives.

In this study, we synthesized the diaminophenyladamantane derivatives, including 1,3-bis(4-aminophenyl) adamantane (1,3-DPANH_2), 2,2-bis(4-aminophenyl)adamantane (2,2-DPANH_2), 1,3-bis(4-(4-aminophenoxy)phenyl) adamantane (1,3-DPAONH_2), 2,2-bis(4-(4-aminophenoxy) phenyl)adamantane (2,2-DPAONH_2), 1,3-bis(4-(4-amino-3-hydroxyphenoxy)phenyl)adamantane (1,3-DPA/OH/NH_2), 2,2-bis(4-(4-amino-3-hydroxyphenoxy)phenyl)adamantane (DPA) and 1,3-bis(4-(4-amino-2-trifluoromethylphenoxy) phenyl)adamantane (1,3-DPA/CF_3/NH_2). The *in vitro* anticancer activities of those compounds were screened against the National Cancer Institute (NCI)'s 60 human cancer cell lines. In addition, we characterized the cell cycle progression of DPA in Colo 205, HCT-15 and HT-29 colon cancer cells. We also evaluated the *in vivo* anticancer activity of DPA in human colon cancer cells Colo 205 xenografts.

Materials and methods

Materials

2,2-DPANH_2 [16] and 2,2-DPAONH_2 [17] were synthesized according to a procedure reported elsewhere. 1,3-DPANH_2 [18], 1,3-DPAONH_2 [19], 1,3-DPA/OH/NH_2 (unpublished data) and DPA (unpublished data) were prepared according to our previous methods. 1,3-Bis(4-hydroxyphenyl)adamantane was synthesized from 1,3-dibromoadamantane and phenol according to our previous method [19].

General methods

A Bio-Rad FTS-40 FTIR spectrophotometer was used to record spectra of the KBr pellets. MS spectra were obtained using a JEOL DMS-D300 mass spectrometer. ^{1}H- and ^{13}C-NMR spectra were recorded on a Bruker AM-400 Fourier transform nuclear magnetic resonance spectrometer using tetramethyl silane (TMS) as the internal standard. A Perkin-Elmer 240C elemental analyzer was used for the elemental analysis.

Synthesis of 1,3-bis(4-(4-nitro-2-trifluoromethylphenoxy)phenyl)adamantane

A mixture of 1,3-bis(4-hydroxyphenyl)adamantane (2.0 g, 6.25 mmol), 2-chloro-5-nitrobenzotrifluoride (3.09 g, 13.7 mmol), potassium carbonate (2.0 g, 14.5 mmol) and 50 ml of dry *N*,*N*-dimethylformamide (DMF) was refluxed at 120°C for 12 h under nitrogen. The reaction mixture was allowed to cool to room temperature and then poured into distilled water. The precipitate was collected by filtration to afford 4.02 g (92.1%) of pale yellow crystals: m.p. 201–203°C; IR(KBr) 3050, 2864, 1595, 1533, 1485 cm^{-1}; MS(EI) *m/z* 698(M^+, 35), 296(100); ^{1}H-NMR(400 MHz, $CDCl_3$) δ 1.82 (s, 2H, H-5,7), 1.99 (s, 8H, H-4, 8, 9, 10), 2.05 (s, 2H, H-6), 2.37 (s, 2H, H-2), 6.93 (d, 2H, ArH), 7.06 (d, 4H, ArH), 7.48 (d, 4H, ArH), 8.25 (d, 2H, ArH), 8.55 (s, 2H, ArH); Crystal data: $C_{36}H_{28}F_6N_2O_6$, pale-yellow crystal, 0.1 × 0.15 × 0.2 mm, triclinic P1 with $a = 9.7213(2)$ Å, $b = 11.4172(2)$ Å, $c = 14.8813(2)$ Å, $\alpha = 91.6850(10)°$, $\beta = 105.18°$, $\gamma = 91.5670(10)°$ with $D_c = 1.457$ g/cm^3 for $Z = 2$, $V = 1592.28(56)$ Å^3, $T = 296$ K, $\lambda = 0.71013$ Å, $F(000) = 720$. Anal. calcd for $C_{36}H_{28}F_6N_2O_6$:C, 61.89; H, 4.01; N, 4.01. Found: C, 61.82; H, 4.05; N, 3.98.

Scheme 1

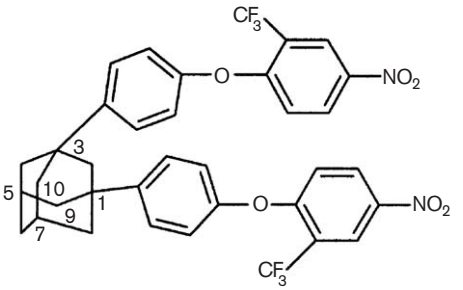

Synthesis of 1,3-bis(4-(4-amino-2-trifluoromethylphenoxy)phenyl)adamantane

A 150-ml, three-necked, round-bottomed flask was charged with 1,3-bis(4-(4-nitro- 2-trifluoromethylphenoxy)phenyl)adamantane (2.00 g, 2.86 mmol), 100 ml of ethanol, and 0.08 g of 10% palladium on carbon (Pd-C). The mixture was heated to reflux and hydrazine monohydrate (40 ml) was added dropwise to the mixture. After a further 24 h reflux, the catalyst was removed by hot filtration. The filtrate was poured into 50 ml of water to give 1.50 g (82.1%) of off-white powder: m.p. 153–154°C; IR(KBr) 3460, 3377, 2890, 2870, 1630, 1497 cm^{-1}; MS(EI) *m/z* 638(M^+, 8), 266(55), 176(100); ^{1}H-NMR(400 MHz, DMSO-d_6) δ 1.69 (s, 2H, H-5,7), 1.79–1.86 (m, 10H, H-4, 6, 8, 9, 10), 2.20 (s, 2H, H-2), 5.42 (s, 4H, NH_2), 6.77–6.83 (m, 8H, ArH), 6.91(s, 2H, ArH), 7.31(d, 4H, ArH). Anal. calcd for $C_{36}H_{32}F_6N_2O_2$:

C, 67.71; H, 5.01; N, 4.39. Found: C, 67.65; H, 5.06; N, 4.32.

The NCI's anticancer drug screen

A total of 60 human cancer cell lines were used for the NCI's anticancer drug screen, including the sub-panels of leukemia, melanoma and cancers of lung, colon, brain, ovary, renal, breast and prostate. These cell lines were adaptable to a single growth medium, and had reproducible profiles for growth and drug sensitivity. Detailed methods were described in the literature [20].

Cell culture and DPA treatment

Three colon cancer cell lines Colo 205 (ATCC: CCL-222), HT-29 (ATCC: HTB-38) and HCT-15 (ATCC: CCL-225) were used in this study. Colo 205 cells were cultured in RPMI-1640 with 10% fetal bovine serum (Hyclone, Logan, UT). HT-29 cells were cultured in McCoys 5A with 10% fetal bovine serum and 0.01 mg/ml gentamycin (Gibco, Grand Island, NY). HCT-15 cells were cultured in RPMI-1640 with 20% fetal bovine serum and 0.01 mg/ml gentamycin. Cells were incubated in a humidified atmosphere of 5% CO_2 in air at 37°C. DPA was dissolved in DMSO at a stock concentration of 10 mM and added to culture media at a final concentration of 1–8 μM. Cells were seeded at 5×10^5 cells per T25 culture flask (Corning Glass Works, Corning, NY) in growth medium. The following day the cells were replenished with medium containing the DPA. Cells were harvested and counted by hemocytometry at 24, 48 and 72 h after treatment with DPA, and used for further analysis.

DNA staining

Cycle Test Plus DNA Reagent Kit (Becton Dickinson, San Jose, CA) was used for DNA staining. After washing the cells twice with buffer solution, the cell concentration was adjusted to 1.0×10^6/ml and 0.5 ml of cell suspension was centrifuged at 400 *g* for 5 min at room temperature (20–25°C). The cell pellet was added on 250 μl of Solution A (trypsin buffer) and gently mixed. After incubation at room temperature for 10 min, 200 μl of Solution B (trypsin inhibitor and RNase buffer) was added to each tube, gently mixed and then incubated at room temperature for 10 min. This was followed by with the addition of 200 μl of Solution C [propidium iodide (PI) stain solution] and incubated for 10 min in the dark on ice (2–8°C). The sample was filtered through a 50-mm nylon mesh and used for flow cytometric analysis.

Flow cytometry

Cells (20 000) were analyzed on a FACSCalibur flow cytometer (Becton Dickinson) using an argon ion laser (15 mW) with the incident beam at 488 nm. The red fluorescence (PI) was collected through a 585-nm filter. The data were analyzed using ModFit and CellQuest software on Macintosh computer.

Analysis of the reversibility of DPA-induced growth inhibition of Colo 205 cells

Cells (5×10^5/flask) were seeded on T25 culture flasks and allowed to attach overnight, and then the medium was discarded and replenished with medium containing the DPA for incubation at 37°C for 72 h. At the end of 72 h, the medium was discarded and the cells were replenished with fresh medium. Cells were harvested, and cell viability was examined by hemocytometry at 48 and 72 h after withdrawal from 1, 2, 4 or 8 μM DPA treatment for 72 h.

Antitumor activity of DPA in the ICR nude mice tumor xenograft model

The *in vivo* experiments were carried out with ethical committee approval and meet the standards required by the UKCCCR guidelines [21]. The 8-week-old male ICR nude mice were obtained from the National Laboratory Animal Center of National Applied Research Laboratories (Taipei, Taiwan), and housed in a laminar flow room under sterilized condition with temperature maintained at 25°C and light controlled at 12 h light/12 h dark. Colo 205 cells were harvested and resuspended in serum-free RPMI-1640 medium. Cells were adjusted to 1×10^7 cells/ml and inoculated in nude mice. Each experimental group included seven to eight mice bearing tumors. DPA was dissolved in DMSO and treatment started when tumor size was 2-4 mm. DPA was administered via i.p. injection once a week at doses of 20, 40 or 80 mg/kg (volume of injection:0.1 ml/30 g of body weight), respectively. The control group received DMSO vehicle. Tumor size and body weight were monitored twice a week throughout the experiment. The tumor size was measured using a vernier caliper. Tumor size (V) was calculated according to the following formula: V (mm^2) = $\pi \cdot (A/2 \cdot B/2)$, where A and B are the longest diameter and the shortest diameter, respectively [22]. At day 35, all mice were sacrificed by CO_2 gas. Tumors, livers, kidneys and lungs were collected, fixed, embedded and stained with hematoxylin & eosin for pathological analysis.

Statistics

All data are expressed as mean ± SE. The difference between groups was assessed using Student's t-test. A $p < 0.05$ is considered as a significant difference.

Results and discussion

Chemistry

In order to systematically evaluate the structure–anticancer activity relationship (SAR) of adamantane derivatives, seven adamantane derivatives were synthesized. A novel 1,3-DPA/CF_3/NH_2 was synthesized from

1,3-bis(4-hydroxyphenyl)adamantane in two steps. Reaction of 1,3-bis(4-hydroxyphenyl)adamantane with 2-chloro-5-nitrobenzotrifluoride in anhydrous DMF in the presence of potassium carbonate as an acid acceptor gave 1,3-bis(4-(4-nitro-2-trifluoromethylphenoxy)-phenyl)adamantane (1,3-DPA/CF_3/NO_2), which was hydrogenated to give 1,3-DPA/CF_3/NH_2. The yield of 1,3-DPA/CF_3/NO_2 was high at 92.1% by condensation of 2-chloro-5-nitrobenzotrifluroide with the dipotassium salt of 1,3-dihydroxyadamantane. This high yield can be attributed to the fact that the dipotassium salt of 1,3-dihydroxyadamantane is a good nucleophilic compound due to the adamantly group's electrodonating effect. X-ray diffraction analysis confirmed the structure of 1,3-DPA/CF_3/NO_2. X-ray crystal data for 1,3-DPA/CF_3/NO_2 was acquired from a single crystal, as obtained by slowly crystallizing from the acetone solution. When the nitro compound was converted into 1,3-DPA/CF_3/NH_2, the signal in ^{1}H-NMR appearing at 5.42 p.p.m. is peculiar to the amino group. The elemental analysis, characteristic peaks in the NMR spectra and characteristic bands in the IR spectra confirmed all compounds reported herein.

In vitro anticancer activity of 1,3-substituted diaminophenyladamantane derivatives

For comparison of anticancer activities of the 1,3-substituted adamantane derivatives, 1,3-DPANH_2, 1,3-DPAONH_2, 1,3-DPA/OH/NH_2 and 1,3-DPA/CF_3/NH_2 were synthesized (Fig. 1). Those compounds were submitted to the National Cancer Institute for anticancer assay in culture against a standard panel of cell lines. The results of growth inhibition assays using a number of lines of different tissue origin are given in Table 1. The IC_{50}s of 1,3-DPANH_2 and 1,3-DPAONH_2 were found to be $< 10\,\mu M$ against three (6%) and 32 (60%) cell lines, respectively. Comparison of anticancer activities of 1,3-DPANH_2 and 1,3-DPAONH_2 indicated that 1,3-DPAONH_2 exhibited stronger growth inhibitory on anticancer activities than 1,3-DPANH_2. The results suggest that the configuration of 1,3-DPAONH_2 plays a prominent role in their anticancer activities. We wanted to further confirm that the different substituents (CF_3 and OH) on the phenyl ring of 1,3-DPAONH_2 affect the growth inhibition of cancer cells. The IC_{50}s of 1,3-DPA/CF_3/NH_2 and 1,3-DPA/OH/NH_2 were found to be $< 5\,\mu M$ against 0 (0%) and 47(89%) cell lines, respectively, suggesting that the OH group was favorable for anticancer activities, whereas the CF_3 group was unfavorable. The transformations of 1,3-DPAONH_2 to 1,3-DPA/OH/NH_2 led to a remarked enhancement of anticancer activity toward all the tested cancer lines. The role of the OH group at the *ortho* position of the NH_2 on growth inhibition is remarkable. In addition, one compound (1,3-DPA/OH/NH_2) was confirmed to have an IC_{50} of $< 1\,\mu M$ against one of the cells (BT-549 breast carcinoma). Comparing the anticancer activities of 1,3-substituted diaminophenyladamantane derivatives, the following order of potency against the tested cancer lines was observed: 1,3-DPA/OH/NH_2 > 1,3-DPAONH_2 > 1,3-DPANH_2 > 1,3-DPA/CF_3/NH_2.

In vitro anticancer activity of 2,2-substituted diaminophenyladamantane derivatives

For comparison of anticancer activities of the 2,2-substituted adamantane derivatives, 2,2-DPANH_2, 2,2-DPAONH_2 and DPA were synthesized (Fig. 1). The results of growth inhibition of those compounds *in vitro* against NCI human cancer cell lines are given in Table 2. The IC_{50}s of 2,2-DPANH_2 and 2,2-DPAONH_2 were found to be $< 10\,\mu M$ against nine (17%) and 40 (75%) cell lines, respectively. Comparison of anticancer activities of 2,2-DPANH_2 and 2,2-DPAONH_2 indicated that 2,2-DPAONH_2 exhibited stronger growth inhibitory on anticancer activities than 2,2-DPANH_2. In addition, the transformations of 2,2-DPAONH_2 to DPA led to a remarkable enhancement of anticancer activity toward all the tested cancer lines. The role of the OH group at the *ortho* position of the NH_2 on growth inhibition is remarkable. The IC_{50} of DPA was found to be $< 3\,\mu M$ against 48 (91%) cell lines. Interestingly, one compound (2,2-DPANH_2) was found to have an $IC_{50} < 0.1\,\mu M$ against three of the cells (KM 12 colon, SF-295 CNS and NCI/ADR-RES breast carcinoma). Comparing the anticancer activities of 2,2-substituted diaminophenyladamantane derivatives, the following order of potency against the tested cancer lines was observed: DPA > 2,2-DPAONH_2 > 2,2-DPANH_2. Comparison of anticancer activities of 1,3- and 2,2-substituted diaminophenyladamantane derivatives indicated that 2,2-substituted adamantane derivatives exhibited stronger growth inhibitory on anticancer activities than the corresponding 1,3-substituted analogs (Tables 1 and 2). We noted that 1,3-DPA/OH/NH_2 and DPA exhibited strong growth inhibitory activities *in vitro* against the tested cancer cell lines.

Cell cycle analysis

The cell cycle progression of Colo205, HT 29 and HCT-15 cells was examined using flow cytometry after exposure to 1, 2, 4 or 8 μM DPA for 72 h. Table 3 shows that majority of Colo 205 cells accumulated in G_1 phase (84.1–87.1%) with a decrease of cells in S phase (7.8–10.3%) and G_2/M phase (5.1–5.6%) after treatment with 2 μM DPA for 48–72 h. HT-29 cells were mainly in G_0/G_1 phase (84.1–86.0%) and only a few percent of cells in S phase (7.4–8.0%) after exposure to 4 μM DPA for 48–72 h. The obviously decreased G_2/M phase (6.9–7.6%) of HCT-15 cell populations was observed after their exposure to 8 μM DPA for 24–48 h. The G_0/G_1 arrest was not induced in the HCT-15 cells treated with 1–8 μM DPA for 24–72 h. These results showed that the cell cycle progression in DPA-treated cell lines was

Fig. 1

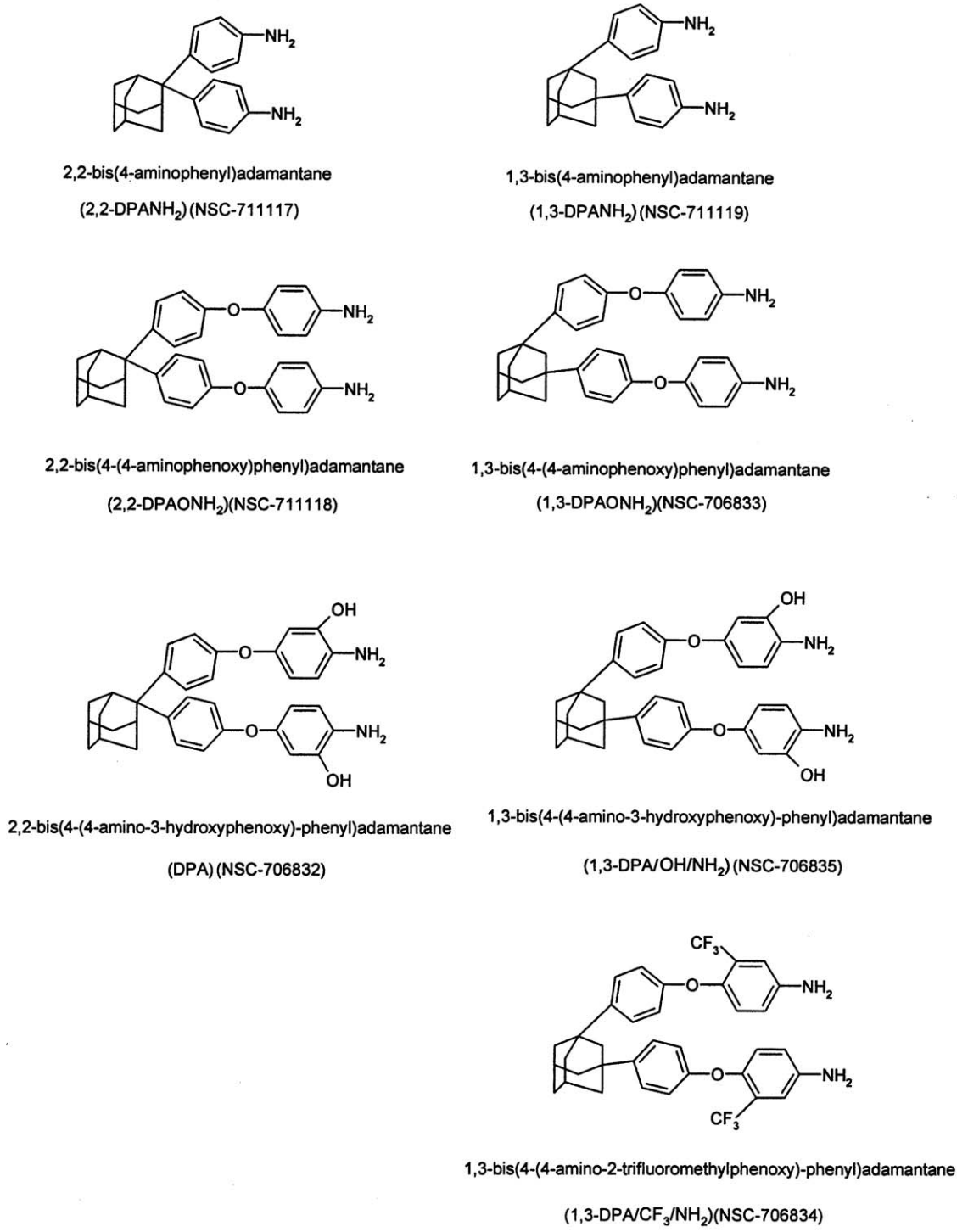

Chemical structures of diaminophenyladamantane derivatives.

heterogeneous. Treatment of Colo 205 and HT-29 cells with DPA resulted in increased G_0/G_1 phase with a concomitant decrease of cells in S phase. DPA exerted a dose-specific effect for the induced G_0/G_1 arrest on Colo 205 cells. The multidrug-resistant HCT-15 showed a different pattern of the cell cycle histogram from the

Table 1 ***In vitro*** **anticancer activity [IC_{50} (μM)[a]] of 1,3-substituted diaminophenyladamantane (NCI panel)**

Cell line	$DPANH_2$	$DPAONH_2$	$DPA/OH/NH_2$	$DPA/CF_3/NH_2$
Leukemia				
CCRF-CEM	15.7	4.83	–[b]	36.2
HL-60(TB)	30.9	17.1	2.12	24.2
K-562	14.6	7.08	3.46	43.9
MOLT-4	11.3	3.81	2.42	35.7
RPMI-8226	10.7	4.14	2.54	–[b]
NSCLC				
A549/ATCC	>100	10.3	1.52	19.0
EKVX	36.6	15.6	1.68	15.4
HOP-62	60	10.7	5.53	18.2
NCI-H226	11.5	23.2	5.05	19.4
NCI-H23	59.6	6.92	1.86	17.7
NCI-H322M	–[b]	8.84	1.26	20.1
NCI-H522	–[b]	13.3	1.40	14.4
Colon cancer				
COLO 205	2.30	13.3	1.84	19.1
HCT-116	44.3	5.65	1.39	24.9
HCT-15	14.5	4.99	1.76	31.8
HT-29	–[b]	7.12	–[b]	17.2
KM-12	>100	4.07	1.72	21.0
SW-620	3.14	6.52	2.89	36.3
CNS cancer				
SF-268	45.2	5.60	1.16	17.4
SF-295	16.4	6.91	2.29	25.3
SNB-19	37.8	8.66	1.31	22.5
U251	14.3	7.90	1.30	14.5
Melanoma				
LOX IMVI	>100	2.44	1.64	17.9
MALME-3M	–[b]	14.6	1.93	22.2
M14	37.1	9.62	1.59	16.9
SK-MEL-2	35.9	15.7	2.45	14.1
SK-MEL-28	15	18.8	2.74	43.2
SK-MEL-5	13.1	13.8	1.88	22.0
UACC-257	75.5	12.5	2.23	18.7
UACC-62	29	9.64	2.65	22.1
Ovarian cancer				
IGROV1	>100	2.64	1.38	19.5
OVCAR-3	48.5	3.08	1.85	17.9
OVCAR-4	10.2	6.98	2.02	36.6
OVCAR-5	27.6	19.1	–[b]	27.0
OVCAR-8	85.1	4.82	2.03	16.0
Renal cancer				
786-0	38.5	8.09	2.83	31.5
A498	15.7	18.0	4.54	18.3
ACHN	41.1	11.7	1.61	32.9
CAKI-1	>100	12.1	1.82	28.1
RXF-393	–[b]	7.78	1.61	11.1
SN12C	25.1	5.76	1.74	31.1
TK-10	>100	24.9	5.57	16.1
UO-31	4.87	13.6	1.95	39.1
Prostate cancer				
PC-3	–[b]	11.5	1.94	14.8
DU-145	51.2	6.41	1.72	35.2
Breast cancer				
MCF-7	31.9	2.89	1.85	13.4
NCI/ADR-RES	56.8	8.59	2.32	21.7
MDA-MB-231	19.6	16.9	1.62	15.2
HS 578T	–[b]	11.7	1.63	17.1
MDA-MB-435	–[b]	5.22	1.92	24.2
MDA-N	37.7	4.33	1.58	36.7
BT-549	42.8	4.02	0.565	21.9
T-47D	–[b]	5.67	1.66	15.1

[a]Cells in RPMI-1640 medium containing 2 mM L-glutamine and 5% fetal bovine serum (heat-inactivated) were exposed to drug for the last 48 h of a 72-h incubation at 37°C in a 5% CO_2 humidified atmosphere and then stained for total protein with sulforhodamine B as described [20].
[b]Not determined.

Table 2 ***In vitro*** **anticancer activity [IC_{50} (μM)[a]] of 2,2-substituted diaminophenyladamantane (NCI panel)**

Cell line	$DPANH_2$	$DPAONH_2$	DPA
Leukemia			
CCRF-CEM	3.76	3.03	3.08
HL-60(TB)	19.2	5.00	2.05
K-562	10.3	3.89	1.98
MOLT-4	4.96	4.27	1.45
RPMI-8226	–[b]	3.01	1.92
NSCLC			
A549/ATCC	–[b]	3.38	1.94
EKVX	16.4	4.76	2.63
HOP-62	13.6	11.8	2.11
NCI-H226	12.4	21.4	1.94
NCI-H23	19.9	5.15	1.84
NCI-H322M	–[b]	0.184	1.41
NCI-H522	15.6	4.28	1.60
Colon cancer			
COLO 205	–[b]	2.71	0.484
HCT-116	20.9	2.71	1.58
HCT-15	21.9	4.94	1.67
HT-29	0.1	2.96	1.81
KM-12	0.01	3.55	2.02
SW-620	11.4	5.03	1.63
CNS cancer			
SF-268	1.57	6.44	1.62
SF-295	0.059	6.76	2.57
SNB-19	14.6	10.1	3.01
U251	18.6	2.81	1.70
Melanoma			
LOX IMVI	16.2	2.75	1.69
MALME-3M	–[b]	13.6	2.02
M14	14.9	2.28	1.69
SK-MEL-2	18.5	16.8	1.69
SK-MEL-28	14.9	10.5	1.68
SK-MEL-5	–[b]	8.38	1.56
UACC-257	19.2	5.76	2.32
UACC-62	16.3	17.7	3.21
Ovarian cancer			
IGROV1	9.6	5.88	1.75
OVCAR-3	10.9	2.58	1.56
OVCAR-4	14.3	6.96	3.07
OVCAR-5	15.8	15.3	2.08
OVCAR-8	7.73	5.82	1.68
Renal cancer			
786-0	–[b]	3.07	1.88
A498	21	2.91	4.67
ACHN	18.6	13.4	1.78
CAKI-1	15	11.1	2.32
RXF-393	2.74	–[b]	1.82
SN12C	18.6	3.65	1.83
TK-10	18	14.3	2.16
UO-31	18.3	3.02	1.85
Prostate cancer			
PC-3	14.9	6.75	1.60
DU-145	–[b]	3.31	2.06
Breast cancer			
MCF-7	19.4	3.81	1.93
NCI/ADR-RES	0.079	15.8	2.33
MDA-MB-231	17.4	17.0	1.82
HS 578T	–[b]	4.91	2.35
MDA-MB-435	14.7	6.04	2.30
MDA-N	18.6	2.74	2.14
BT-549	11.2	4.28	2.05
T-47D	14.4	–[b]	4.13

[a]Cells in RPMI-1640 medium containing 2 mM L-glutamine and 5% fetal bovine serum (heat-inactivated) were exposed to drug for the last 48 h of a 72-h incubation at 37°C in a 5% CO_2 humidified atmosphere and then stained for total protein with sulforhodamine B as described [20].
[b]Not determined.

Colo 205 and HT-29 after DPA treatment. In addition, we noted that DPA-mediated accumulation of Colo 205 and HT-29 cells in G_1 phase (> 80%) was similar to that of DPD. It is likely that the induced G_1 arrest without concomitant apoptosis on Colo 205 and HT-29 colon cancer cells is one unique property of Structure 1. G_1 phase of the cell cycle is an important period where various signals interact to determine the proliferation, quiescence, differentiation or apoptosis of cells [4,5]. Interestingly, DPA exerted G_0/G_1 cell cycle arrest, but not obvious apoptotic-inducing activities in human colon cancer cells lines. Thus, we infer that the induced differentiation of DPA-treated colon cancer cells is possible. The differentiation inducing effect of DPA on colon cancer cells will be further examined.

The irreversible effect of DPA-induced growth inhibition of Colo 205

To further investigate whether the DPA-induced growth inhibition was reversible, Colo 205 cells were treated with DPA for 72 h and the cells were withdrawn from DPA by culturing in fresh medium for another 24 or 48 h. As shown in Figure 2(A) at 24–48 h after removal of 1 μM DPA from the medium the proliferation activity of Colo 205 was reversed and returned to control levels. However, no reversal effect was observed after 2, 4 or 8 μM DPA treatment. The viabilities of treated or non-treated cells were > 80%, except the cells after 8 μM DPA treatment (Fig. 2B). These results showed DPA could induce an irreversible antiproliferative effect on Colo 205 cells and this property was also similar to that of DPD [14]. These results highlight the important properties of irreversible anticancer activity of adamantane and diamantane derivatives. One possibility is that the relatively lipophilic nature of DPA or DPD reduced cellular efflux after the initial drug exposure. We infer that the irreversible property of adamantane and diamantane derivatives provides an advantage to prolong the anticancer activity.

Structure 1

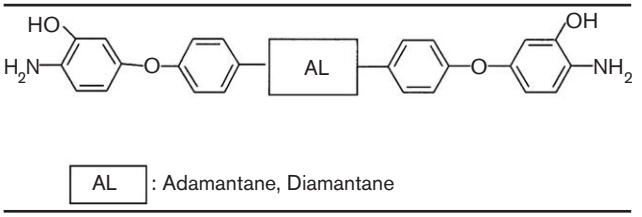

In vivo antiproliferation effect of DPA for human colon cancer xenografts

We further examined whether DPA is also effective *in vivo* after tumor formation. For comparison of the *in vivo* antitumor activity with DPD (DPA analog), we followed the method of our previous study [15] and similar doses were used. Cancer cells were transplanted into ICR nude mice and when the tumors were palpable (2–4 mm), the mice were treated either with vehicle control or DPA (20–80 mg/kg, i.p., once a week). After treatment of nude mice with DPA (40 mg/kg), the tumor size (mm^2) was significantly ($p < 0.05$) decreased in mice as compared to control groups. Figure 3(A) shows that tumor size from control animals showed an average of 81.5 mm^2 at the end of this study. In contrast, the tumor size from DPA (40 mg/kg)-treated animals had an average of only 29.6 mm^2. The tumor size of DPA-treated animals (20 and 80 mg/kg) was not significantly decreased compared to the vehicle control at the end point. While treatment of the *in vivo* Colo 205 model at 40 mg/kg led to an apparent decrease in tumor size, exposure to 80 mg/kg apparently did not (Fig. 3A). The result might be explained by the two possible causes. (i) One mouse

Table 3 The effect of DPA on cell cycle progression in three colon cancer cell lines[a]

Time (h)	Concentration (μM)	Colo 205			HT-29			HCT-15		
		G_0/G_1 (%)	S (%)	G_2/M (%)	G_0/G_1 (%)	S (%)	G_2/M (%)	G_0/G_1 (%)	S (%)	G_2/M (%)
24	control	53.7[b]	33.1	13.2	50.8	38.8	10.5	36.8	44.1	19.0
	1	58.9	29.0	12.0	56.6	33.1	10.3	31.4	50.6	18.1
	2	67.1	24.1	48.3	67.0	23.1	10.0	31.8	54.0	14.2
	4	67.5	24.3	8.2	72.1	17.1	10.9	30.6	58.2	11.2
	8	70.5	24.3	5.2	77.0	13.3	9.6	39.6	53.5	6.9
48	control	54.8	35.9	9.3	59.3	31.5	9.3	43.9	40.3	15.8
	1	53.3	39.0	7.6	61.6	29.0	9.4	39.1	45.1	15.8
	2	84.1	10.3	5.6	77.5	17.8	4.7	35.2	48.8	16.0
	4	71.6	18.1	10.4	84.1	7.4	8.5	30.5	55.3	14.3
	8	70.6	24.1	5.2	79.5	10.6	10.0	37.5	54.9	7.6
72	control	62.0	28.1	9.8	75.9	17.6	6.5	58.0	32.1	9.8
	1	60.3	29.6	10.1	72.6	20.1	7.3	51.8	35.0	13.2
	2	87.1	7.8	5.1	67.3	29.9	2.9	49.2	36.6	14.3
	4	76.3	13.4	10.3	86.0	8.0	6.1	40.8	42.1	17.2
	8	70.7	25.8	3.4	86.3	7.5	6.2	38.2	49.9	11.9

[a]The cell cycle progression of Colo 205, HT-29 and HCT-15 cells was examined after exposure to DPA for 24, 48 or 72 h.
[b]Data are the mean of duplicate samples from one of three independent experiment.

Fig. 2

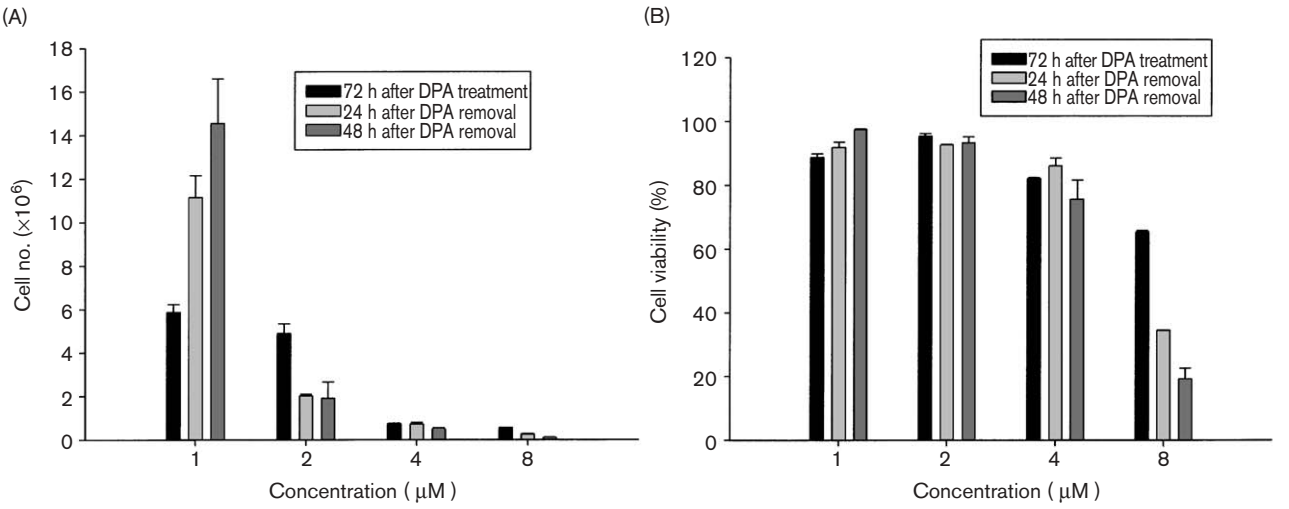

(A) The irreversible effect of DPA-induced growth inhibition of Colo 205. Cells were seeded at 5×10^5 cells per T25 culture flasks in growth medium. The following day the cells were replenished with medium containing 1, 2, 4 or 8 μM DPA. Cells were harvested at days 1 and 2 after 1, 2, 4 or 8 μM DPA treatment for 72 h, then withdrawal. (B) Cell viability was examined by hemocytometry. Each point represents the mean ± SE of duplicate cultures.

Fig. 3

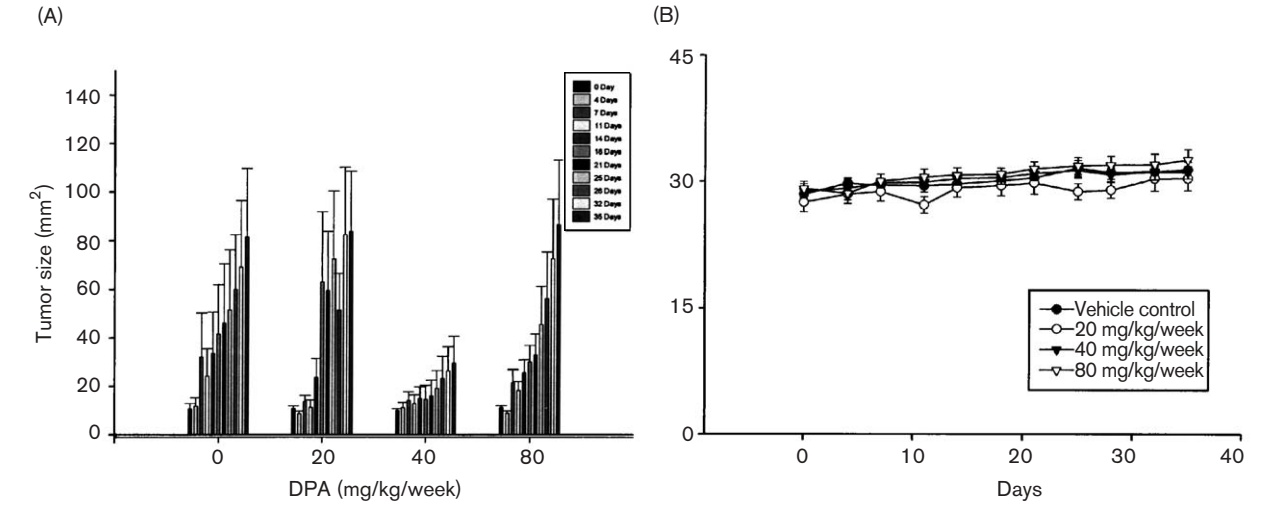

(A) The *in vivo* antiproliferative effect of DPA for human colon cancer Colo 205 xenografts. When the tumors were palpable (2–4 mm), the ICR nude mice were either treated with vehicle control or DPA (i.p., once a week). Each data are the mean ± SE from seven to eight samples of one representative experiment. Treatment of nude mice with DPA (40 mg/kg/week), the tumor size was significantly ($p < 0.05$) decreased in mice as compared to control groups. (B) Changes in body weight of nude mice after treatment with DPA. Each data point is the mean ± SE from seven to eight samples of one representative experiment.

had an abnormally large tumor size among the DPA 80 mg/kg-treated mice. Its tumor size (48.6 mm^2) was about 3-fold larger than the average tumor size (16.7 mm^2) of the other DPA 80 mg/kg-treated mice at 7 days after the initial treatment. This result may be due to the idiopathic property of the mouse. (ii) DPA presented the dose-specific effect for antitumor activity on human colon cancer xenografts. The dose-specific

phenomenon was also found in the *in vitro* study of DPA-induced cell cycle arrest on Colo 205 cells (Table 3). We suggest that the concentration of maximum effect of DPA-induced *in vivo* antitumor effect is about 40 mg/kg/week and this effective dose is similar to DPD (15). The challenge of DPA (20-80 mg/kg, i.p., once a week) in nude mice throughout the experiment produced no obvious acute toxicity. No significant reduction in body weight was found in DPA-treated mice (Fig. 3B). These results show the less toxic property of DPA.

Conclusion

Herein we described the *in vitro* and *in vivo* anticancer profile of diaminodiphenyladamantane derivatives. 2,2-Substituted adamantane derivatives exhibited stronger growth inhibitory on anticancer activities *in vitro* than the corresponding 1,3-substituted analogs. DPA and 1,3-DPA/OH/NH_2 were potent growth inhibitors of cancer cell lines *in vitro*. DPA also exerted G_0/G_1 cell cycle arrest without concomitant apoptosis on Colo 205 and HT-29 colon cancer cells. The result was similar to that of DPD. In other words, induced G_1 arrest without concomitant apoptosis on Colo 205 and HT-29 colon cancer cells is a unique property of DPD and DPA. In addition, the *in vivo* effect of tumor growth suppression by DPA was also observed on colon Colo 205 xenografts. No acute toxicity was observed after an i.p. challenge of DPA in ICR nude mice, weekly. These results suggest that DPA may be a novel less toxic modality of cancer therapy.

Acknowledgments

The authors are grateful to Drs Ven L. Narayanan, Edward Sausville, Yali F. Hallock, Anthony B. Mauger and Robert J. Schultz at the NCI for kind assistance. We are grateful to the National Science Council of the Republic of China for the support of this work.

References

1 Giovannucci E. Modifiable risk factors for colon cancer. *Gastroenterol Clin N Am 2002;* **31**:925–943.
2 NIH Consensus Conference. Adjuvant therapy for patients with colon and rectal cancer. *J Am Med Ass* 1990; **19**:1444–1448.
3 Hung DT, Jamison TF, Schreiber SL. Understanding and controlling the cell cycle with natural products. *Chem Biol* 1996; **3**:623–639.
4 Sherr CJ. Cancer cell cycles. *Science* 1996; **274**:1672–1677.
5 Sherr CJ. G_1 phase progression: cycling on cue. *Cell* 1994; **79**: 551–555.
6 Aigami K, Inamoto Y, Takaishi N, Hattori K. Biologically active polycycloalkanes. 1. Antiviral adamantine derivatives. *J Med Chem* 1975; **18**:713–721.
7 Tverdislov VA, el-Karadagi S, Kharitonenkov IG, Glaser R, Donath E, Herrmann A, *et al.* Interaction of the antivirus agents remantadine and amantadine with lipid membranes and the influence on the curvature of human red cells. *Gen Physiol Biophys* 1986; **5**:61–75.
8 Chen HSV, Pellegrini JW, Aggarwal SK, Lei SZ, Warach S, Jensen FE, *et al.* Open-channel block of *N*-methyl-D-aspartate (NMDA) responses by memantine: therapeutic advantage against NMDA receptor-mediated neurotoxicity. *J Neurosci* 1992; **12**:4427–4436.
9 Kornhuber J, Bormann J, Hubers M, Rusche K, Riederer P. Effects of the 1-amino-adamantanes at the MK-801-binding site of the NMDA-receptor-gated ion channel: a human postmortem brain study. *Eur J Pharmacol* 1991; **206**:297–300.
10 Donath E, Herrmann A, Coakley WT, Groth T, Egger M, Taeger M. The influence of the antiviral drugs amantadine and remantadine on erythrocyte and platelet membranes and its comparison with that of tetracaine. *Biochem Pharmacol* 1987; **36**:481–487.
11 Tsuzuki N, Hama T, Kawada M, *et al.* Admantane as a brain-directed drug carrier for poorly absorbed drug. 2. AZT derivatives conjugated with the 1-admantane moiety. *J Pharmac Sci* 1994; **83**:481–484.
12 Wang JJ, Chern YT, Chang YF, Liu TY, Chi CW. Dimethyladamantylmaleimide-induced *in vitro* and *in vivo* growth inhibition of human colon cancer Colo 205 cells. *Anticancer Drugs* 2002; **13**: 533–543.
13 Wang JJ, Chern YT, Liu TY, Chi CW. *In vitro* and *in vivo* growth inhibition of cancer cells by adamantylmaleimide derivatives. *Anticancer Drug Des* 1998; **13**:79–96.
14 Wang JJ, Huang KT, Chern YT. Induction of growth inhibition and G_1 arrest in human cancer cell lines by relatively low toxic diamantane derivatives. *Anticancer Drugs* 2004; **15**:277–286.
15 Wang JJ, Chang YF, Chern YT, Chi CW. Study of the *in vitro* and *in vivo* effects of 1,6-Bis[4-(4-amino-3-hydroxyphenoxy)phenyl]diamantane (DPD), a novel cytostatic and differentiation inducing agent, on human colon cancer cells. *Br J Cancer* 2003; **89**:1995–2003.
16 Yi MH, Huang W, Lee BJ, Choi KY. Synthesis and characterization of soluble polyimides from 2,2-bis(4-aminophenyl)cycloakane derivative. *J Polym Sci Polym Chem* 1999; **37**:3449–3454.
17 Hsiao SH, Li CT. Synthesis and characterization of new adamantane-based polyimides. *Macromolecules* 1998; **31**:7213–7217.
18 Chern YT, Shiue HC. Low dielectric constant polyimides derived from 1,3-bis(4-aminophenyl)adamantane. *Macromol Chem Phys* 1998; **199**: 963–969.
19 Chern YT, Shiue HC. Low dielectric constants of soluble polyimides based on adamantane. *Macromolecules* 1997; **30**:4646–4651.
20 Monks A, Scudiero D, Skehan P, Shoemaker R, Paull K, Vistica D, *et al.* Feasibility of a high-flux anticancer drug screen using a diverse panel of cultured human tumor cell lines. *J Natl Cancer Inst* 1991; **93**: 757–766.
21 Workman P, Twentyman P, Balkwill F, Balmain A, Chaplin D, Double J, *et al.* United Kingdom Co-ordinating Committee on Cancer Research (UKCCCR) guidelines for the welfare of animals in experimental neoplasia (second edition). *Br J Cancer* 1998; **77**:1–10.
22 Gottardis MM, Jiang SY, Jeng MH, Jordan VC. Inhibition of tamoxifen-stimulated growth of an MCF-7 tumor variant in athymic mice by novel steroidal antiestrogens. *Cancer Res* 1989; **49**:4090–4093.